Cooperation of p40^{phox} with p47^{phox} for Nox2-based NADPH Oxidase Activation during Fcγ Receptor (FcγR)-mediated Phagocytosis

MECHANISM FOR ACQUISITION OF p40^{phox} PHOSPHATIDYLINOSITOL 3-PHOSPHATE (PI(3)P) BINDING[*][S]

Received for publication, March 13, 2011, and in revised form, September 27, 2011 Published, JBC Papers in Press, September 28, 2011, DOI 10.1074/jbc.M111.237289

Takehiko Ueyama[‡1], Junya Nakakita[‡], Takashi Nakamura[‡], Takeshi Kobayashi[§], Toshihiro Kobayashi[¶], Jeonghyun Son[‡], Megumi Sakuma[‡], Hirofumi Sakaguchi[‖], Thomas L. Leto[**], and Naoaki Saito[‡2]

From the [‡]Laboratory of Molecular Pharmacology, Biosignal Research Center, Kobe University, Kobe 657-8501, Japan, the [§]Department of Physiology, Nagoya University Graduate School of Medicine, Nagoya 466-8550, Japan, the [¶]Department of Physical Therapy, Kobe International University, Kobe 658-0032, Japan, the [‖]Department of Otolaryngology-Head and Neck Surgery, Kyoto Prefectural University of Medicine, Kyoto 602-8566, Japan, and the [**]Molecular Defenses Section, Laboratory of Host Defenses, National Institute of Allergy and Infectious Diseases, National Institutes of Health, Rockville, Maryland 20852

Background: p40^{phox} acquires PI(3)P-binding capabilities through arachidonic acid-induced and H_2O_2-induced conformational changes in phagocytes.
Results: In addition to conformational changes induced by H_2O_2 in the cytoplasm, p40^{phox} can acquire PI(3)P binding following membrane targeting.
Conclusion: p40^{phox} has novel mechanisms inducing its conformation changes, apart from p47^{phox}.
Significance: This study demonstrates both p40^{phox} and p47^{phox} synchronously function as "carriers" and "adaptors" of Nox2-based NADPH oxidase assembly through their conformation changes.

During activation of the phagocyte (Nox2-based) NADPH oxidase, the cytoplasmic Phox complex (p47^{phox}-p67^{phox}-p40^{phox}) translocates and associates with the membrane-spanning flavocytochrome b_{558}. It is unclear where (in cytoplasm or on membranes), when (before or after assembly), and how p40^{phox} acquires its PI(3)P-binding capabilities. We demonstrated that in addition to conformational changes induced by H_2O_2 in the cytoplasm, p40^{phox} acquires PI(3)P-binding through direct or indirect membrane targeting. We also found that p40^{phox} is essential when p47^{phox} is partially phosphorylated during FcγR-mediated oxidase activation; however, p40^{phox} is less critical when p47^{phox} is adequately phosphorylated, using phosphorylation-mimicking mutants in HEK293$^{Nox2/FcγRIIa}$ and RAW264.7$^{p40/p47KD}$ cells. Moreover, PI binding to p47^{phox} is less important when the autoinhibitory PX-PB1 domain interaction in p40^{phox} is disrupted or when p40^{phox} is targeted to membranes. Furthermore, we suggest that high affinity PI(3)P binding of the p40^{phox} PX domain is critical during its accumulation on phagosomes, even when masked by the PB1 domain in the resting state. Thus, in addition to mechanisms for directly acquiring PI(3)P binding in the cytoplasm by H_2O_2, p40^{phox} can acquire PI(3)P binding on targeted membranes in a p47^{phox}-dependent manner and functions both as a "carrier" of the cytoplasmic Phox complex to phagosomes and an "adaptor" of oxidase assembly on phagosomes in cooperation with p47^{phox}, using positive feedback mechanisms.

In phagocytic cells, reactive oxygen species (ROS)[3] are produced by the phagocyte NADPH oxidase. The enzyme is a multiprotein complex assembled from the membrane-spanning flavocytochrome b_{558} (composed of Nox2 (gp91^{phox}) and p22^{phox}) and four cytoplasmic components (p47^{phox}, p67^{phox}, p40^{phox}, and Rac) (1–3). In unstimulated phagocytes, the oxidase is dissociated and inactive; the flavocytochrome b_{558} is stored on the membranes of intracellular granules (4), and the other Phox proteins associate in a separate cytoplasmic ternary complex (p47^{phox}-p67^{phox}-p40^{phox}) (5) in a dephosphorylated state (6–8). During phagocyte activation, intracellular granules containing flavocytochrome b_{558} fuse to newly forming phago-

* This work was supported in part by the National Institutes of Health, NIAID, Intramural Research Program. This work was also supported in part by Grants-in-aid for scientific research; on the Global Center of Excellence Program, on Priority Areas "Transportsome," on Innovative Areas "Fluorescence Live Imaging" and (C), from the Ministry of Education, Culture, Sports, Science and Technology, Japan. This work was also supported by the "Japan-Hungary Research Cooperative Program" grant from the Japan Society for the Promotion of Science and Hungarian Academy of Sciences, by a grant from the Naito Foundation, by a grant from the Suzuken Memorial Foundation, and by a grant from the Takeda Science Foundation.
[S] The on-line version of this article (available at http://www.jbc.org) contains supplemental Figs. 1–9 and Videos 1–5.
[1] To whom correspondence may be addressed. Tel.: 81-78-803-5962; Fax: 81-78-803-5971; E-mail: tueyama@kobe-u.ac.jp.
[2] To whom correspondence may be addressed. Tel.: 81-78-803-5961; Fax: 81-78-803-5971; E-mail: naosaito@kobe-u.ac.jp.

[3] The abbreviations used are: ROS, reactive oxygen species; EE, early endosome; FcγR, Fcγ receptor; PI(3)P, phosphatidylinositol 3-phosphate; PI(3,4)P_2, phosphatidylinositol 3,4-bisphosphate; PI, phosphoinositide; BIgG, IgG-opsonized glass beads; AIR, autoinhibitory region; PM, plasma membrane; p, prenylation motif; pp, polybasic and prenylation motif; CGD, chronic granulomatous disease; PMA, phorbol 12-myristate 13-acetate; fMLP, formylmethionylleucylphenylalanine; Ab, antibody; pAb, polyclonal antibody; aa, amino acids; EEA1, early endosome antigen-1; mKO, monomeric Kusabira-Orange; EGFP, enhanced GFP; PH, pleckstrin homology.

somes, and the cytoplasmic ternary complex binds to these membranes; p47*^phox^* is phosphorylated (9, 10), thereby inducing conformational changes that promote interaction of the ternary complex with p22*^phox^* (11), and p40*^phox^* also undergoes conformational changes by disruption of the intramolecular PX-PB1 domain interaction to enable the ternary complex to bind through the p40*^phox^* PX domain to PI(3)P (12, 13), which is enriched in phagosomes (14–16).

Chronic granulomatous disease (CGD), characterized by defective microbial killing by phagocytic cells, is caused by defects or deficiencies in any one of five oxidase components: Nox2, p22*^phox^*, p47*^phox^*, p67*^phox^*, or p40*^phox^*. An essential role for Rac in NADPH oxidase activation was also demonstrated in an oxidase-deficient patient who expressed mutated Rac2 (1) and in mice rendered genetically deficient in Rac2 or in Rac1 plus Rac2 (17). p47*^phox^* is called a "carrier," "adaptor," or "organizer" component because it binds to membrane lipids ($PI(3,4)P_2$, phosphatidic acid, and phosphatidylserine) through its PX domain (18), is tethered to the flavocytochrome b_{558} through direct interactions between p22*^phox^* and its tandem SH3 domains, and is linked to other cytoplasmic Phox proteins in this complex (19, 20). CGD patients who lack p47*^phox^* show impaired translocation of p67*^phox^* to the particulate fraction or phagosomes in response to PMA (21, 22), fMLP (22), or opsonized zymosan (23), whereas CGD patients who lack p67*^phox^* show normal translocation of p47*^phox^* to the particulate fraction (21, 22). p40*^phox^* was shown to act as an essential positive regulator of Nox2 in studies in p40*^phox^*-deficient mice (24), in $p40^{phoxR58A/-}$ knock-in mice (25), or in FcγIIa receptor-reconstituted cells (26). In recent work, we described a model in which p47*^phox^* functions as an early stage carrier and adaptor protein of the cytoplasmic ternary complex, whereas p40*^phox^* functions as a late stage carrier or adaptor protein that links the cytoplasmic ternary complex to closed phagosomes and prolongs retention of the complex on phagosomes using PI(3)P binding during FcγR-mediated oxidative burst (12, 27). Although mounting evidence suggested that p40*^phox^* functions as an essential positive regulator of the Nox2-based NADPH oxidase, only recently was p40*^phox^* deficiency described in a CGD patient, who has compound heterozygosity for a missense mutation predicting a R105Q substitution in the PX domain and a frameshift mutation at codon 52 (K52R) with a premature stop at codon 79 and exhibited a severe defect in FcγR-mediated oxidative burst but not in PMA- or fMLP-stimulated extracellular ROS release (28). Contrary to views on the role of p40*^phox^* serving as a carrier of the cytoplasmic Phox complex (12, 27, 29–31), a recent report suggested that p40*^phox^* primarily functions in sustaining Nox2 activity on phagosomes rather than in translocation of the cytoplasmic Phox complex to phagosomes (32). Another report suggested that although p40*^phox^* acts as a carrier of the Phox complex, this function is PX domain-dependent but PI(3)P-independent in PMA-stimulated permeabilized PLB-985 neutrophil cores (31). Thus, where (in the cytoplasm or on membranes), when (before or after assembly), and how p40*^phox^* acquires its PI(3)P-binding capabilities is unsolved, and how p40*^phox^* cooperates with p47*^phox^* during oxidase assembly or activation is also unclear. To address these questions, we used membrane-targeted mutants of p40*^phox^* and p47*^phox^* to delineate contributions of various intra- and intermolecular domain interactions affecting their targeting to phagosomes and oxidase activation. Here we show that in addition to acquiring PI(3)P-binding capabilities following exposure to H_2O_2 in the cytoplasm, p40*^phox^* can acquire PI(3)P binding following membrane targeting, either directly by itself or indirectly in a p47*^phox^*-dependent manner through interactions in the p47*^phox^*-p67*^phox^*-p40*^phox^* complex. We found that the dependence on p40*^phox^* PI(3)P binding for Nox2 activity is determined by the phosphorylation status of p47*^phox^*. p40*^phox^* is essential during FcγR-mediated oxidase activation; however, p40*^phox^* is less critical under conditions when p47*^phox^* is adequately phosphorylated, using phosphorylation/activation-mimicking p47*^phox^* mutants. Moreover, PI binding of p47*^phox^* is less important when the autoinhibitory PX-PB1 domain interaction in p40*^phox^* is disrupted or when p40*^phox^* is targeted to membranes. Taken together, these results indicate that p40*^phox^* and p47*^phox^* cooperate in executing the carrier function directing the cytoplasmic ternary Phox complex to phagosomes and the adaptor function for assembly of the Nox2 complex during the FcγR-mediated oxidative burst.

EXPERIMENTAL PROCEDURES

Materials—Goat polyclonal antibody (pAb) against p47*^phox^* or p67*^phox^* and rabbit pAb against p40*^phox^* were described previously (33, 34). Rabbit pAb against mouse p40*^phox^* and mouse monoclonal Ab (mAb) against p67*^phox^* were from Millipore and BD Biosciences, respectively. Mouse mAb against the C terminus of p47*^phox^* (196–390 aa) and rabbit mAb against the C-terminal end of p40*^phox^* were from Santa Cruz Biosciences and Abcam, respectively. Mouse mAb against gp91*^phox^* or p22*^phox^* was a kind gift from Drs. Roos and Verhoeven (35). Goat pAb against FcγRIIa and mouse mAb against early endosome antigen-1 (EEA1) were from R&D Systems and BD Biosciences, respectively. H_2O_2 was from Wako Pure Chemical Industries.

Cell Culture—HEK293 cells (ATCC) were maintained in Eagle's minimal essential medium (Wako) containing 10% heat-inactivated FBS (Invitrogen), 100 μM nonessential amino acids (Invitrogen), and antibiotics at 37 °C in 5% CO_2. RAW264.7 cells were described previously (36). For establishing clonally derived HEK293 lines with stable expression of human Nox2 and human FcγRIIa ($HEK293^{Nox2/Fc\gamma RIIa}$), Nox2 in pcDNA3.1(Neo) and FcγRIIa in pcDNA3.1(Neo) were transfected into HEK293 cells using FuGENE 6 (Roche Applied Science) and followed by selection in the presence of 1 mg/ml G418 (Calbiochem). Establishment of the cloned lines was confirmed by immunoblotting and immunostaining using α-Nox2 Ab (or α-p22*^phox^* Ab) and α-FcγRIIa Ab (supplemental Fig. 1, *A* and *B*), and by a ROS assay using IgG-opsonized glass beads (BIgG) after transfection of p47*^phox^* + p67*^phox^* with/without p40*^phox^* (supplemental Fig. 1*C*). A clonally derived HEK 293 line with stable expression of human p67*^phox^* ($HEK293^{p67phox}$) was established in the same way as described above (supplemental Fig. 5*A*).

For establishing clonally derived RAW264.7 lines with stable knockdown of p40*^phox^* alone ($RAW264.7^{p40KD}$) or both p40*^phox^* and p47*^phox^* ($RAW264.7^{p40/p47KD}$), empty pSUPER(puro) vector (OrigoEngine) or pSUPER(puro) vector(s) containing a tar-

TABLE 1
Summary of properties of p47^{phox}, p67^{phox}, and p40^{phox} mutants used in the present study

Name of expressed mutant	Properties of expressed protein
p47^{phox}p	Endomembrane-targeted mutant which is adapted with CLLL motif of Rac1 at its C terminus
Noxo1-p47^{phox}	PM-targeted mutant of p47^{phox} in which its PX domain is replaced with the PX domain of Noxo1
Noxo1(R40Q)-p47^{phox}	Noxo1-p47^{phox} with R40Q mutation
p40-p47^{phox}	p47^{phox} mutant in which its PX domain is replaced with the PX domain of p40^{phox}
p40(R105K)-p47^{phox}	p40-p47^{phox} with R105K mutation
p47^{phox}(R90K)	PI binding-deficient and membrane targeting-defective mutant
p47^{phox}(R90K)p	p47^{phox}(R90K) with CLLL motif at its C terminus
p47^{phox}(ΔAIR)	AIR-deleted mutant that constitutively interacts with p22^{phox}
p47^{phox}(S303D), p47^{phox}(S304D), p47^{phox}(S328D)	One-phosphorylation site-mimicking mutants
p47^{phox}(S303D/S304D), p47^{phox}(S303D/S328D), p47^{phox}(S304D/S328D)	Two-phosphorylation site-mimicking mutants
p47^{phox}(S303D/S304D/S328D)	Three-phosphorylation site-mimicking mutant that can interact with p22^{phox}
p67^{phox}(K355A)	p40^{phox} binding-deficient mutant
p67^{phox}pp	PM-targeted mutant that is adapted with a KKRKRK + CLLL motif of Rac1 at its C terminus
p40^{phox}(R105K)	PI(3)P binding-deficient mutant
p40^{phox}(F320A)	Intramolecular PX-PB1 domain interaction-defective mutant
p40^{phox}(R105K/F320A)	p40^{phox}(F320A) with R105K mutation
p40^{phox}pp	PM-targeted mutant that is adapted with a KKRKRK + CLLL motif at its C terminus
p40^{phox}(ΔPX)pp	p40^{phox}pp with deletion of its PX domain
p40^{phox}p	Endomembrane-targeted mutant that is adapted with a CLLL motif at its C terminus
p40^{phox}(R105K)p	p40^{phox}p with R105K mutation
FYVE-p40^{phox}	p40^{phox} mutant in which its PX domain is replaced with the FYVE domain of Hrs
FYVE-p40^{phox}p	FYVE-p40^{phox} with a CLLL motif at its C terminus
PH(TAPP1)-p40^{phox}	p40^{phox} mutant in which its PX domain is replaced with the PH domain of TAPP1

get sequence (three sequences each) was transfected into RAW264.7 cells using FuGENE HD (Promega) and followed by selection in the presence of 1.5 mg/ml puromycin (Wako). Establishment of the cloned lines was confirmed by immunoblotting and ROS assays using BIgG (supplemental Fig. 2). The most efficient target sequence for p40^{phox} knockdown among three tested was GCAAATTGGAGCTAAGTTTCA (nucleotide 554–574 from ATG), and that for p47^{phox} among three tested was GCGAAGAAGCCTGAGACATAC (nucleotide 397–417 from ATG), respectively.

Construction of Plasmids—Human FcγRIIa, a low affinity to IgG and monomeric type of Fcγ receptor, was amplified by PCR using the first-strand cDNA from leukocyte (BD Biosciences) and cloned into XbaI/EcoRI sites of pcDNA3.1 vector (Invitrogen). Human Nox2, p47^{phox}, p67^{phox}, and p40^{phox} in pcDNA3.1 were described previously (12, 27, 37). p67^{phox}(K355A), which does not bind p40^{phox} (29) in pcDNA3.1, was made by site-directed mutagenesis using a QuikChange II XL site-directed mutagenesis kit (Stratagene). GFP-p47^{phox}, GFP-p67^{phox}, GFP-p40^{phox}, and GFP-p40^{phox}(PX) were also described previously (12, 27, 38). For p47^{phox}(ΔAIR: Δ298–340 aa) construction, two fragments (p47^{phox}(1–297 aa) with BamHI/ApaI sites and p47^{phox}(298–390 aa) with ApaI/EcoRI sites) were amplified by PCR and cloned into BamHI/EcoRI sites of pcDNA3.1 or BglII/EcoRI sites of pEGFP(C1) (BD Biosciences). The plasma membrane (PM)-targeted mutant of p67^{phox} (p67^{phox}pp) in pcDNA3.1, which is adapted with the C-terminal, polybasic motif (KKRKRK; 183–188 aa) and isoprenylation motif (CLLL; 189–192 aa) of Rac1, was described previously (37), and GFP-p67^{phox}pp was made by transfer of p67^{phox}pp into BglII/SalI sites of pEGFP(C3). p47^{phox}(R90K), p47^{phox}(S303D), p47^{phox}(S304D), p47^{phox}(S328D), p47^{phox}(S303D/S304D), p47^{phox}(S303D/S328D), p47^{phox}(S304D/S328D), p47^{phox}(S303D/S304D/S328D) in pcDNA3.1 were made using QuikChange. p40^{phox}(R105K), in pcDNA3.1, which does not bind PI(3)P (39), and p40^{phox}(F320A), in pcDNA3.1 or in pEGFP(C1), which disrupts the intermolecular PX-PB1 interaction within p40^{phox} (12, 13, 27), were also made using QuikChange. For Noxo1-p47^{phox} and Noxo1(R40Q)-p47^{phox} construction, two fragments (Noxo1(PX: 1–122 aa) or Noxo1(PX,R40Q) with BamHI/AflII and p47^{phox}(123–390 aa) with AflII/EcoRI) were amplified by PCR (40) and cloned into BamHI/EcoRI sites of pcDNA3.1 or into BglII/EcoRI sites of pEGFP(C1). An endomembrane-targeted mutant of p40^{phox} (p40^{phox}p in pcDNA3.1 or pEGFP(C1)), which is adapted with the isoprenylation motif (CLLL) alone, and the PM-targeted mutant of p40^{phox} (p40^{phox}pp in pcDNA3.1 or pEGFP(C1)), which is adapted with both the polybasic and isoprenylation motif (KKRKRKCLLL), were made using QuikChange. p40^{phox}pp deleted of its PX domain (1–136 aa) (p40^{phox}(ΔPX)pp) with BamHI/EcoRI sites was amplified by PCR and cloned into BglII/EcoRI sites of pEGFP(C1), and GFP-p40^{phox}(R105K)p was made using QuikChange. N-terminally monomeric Kusabira-Orange (mKO; excitation, 548 nm; emission, 561 nm) (27)-tagged p40^{phox} (mKO-p40^{phox}) was made by replacement of EGFP with mKO in pEGFP(C1) vector, and mKO-p40^{phox}(R105K) was made using QuikChange. For FYVE-p40^{phox} construction, two fragments (mouse FYVE domain (147–297 aa) of hepatocyte growth factor-regulated tyrosine kinase substrate (Hrs) (41) with BamHI/NdeI and p40^{phox}(137–341 aa) with NdeI/EcoRI) were amplified by PCR and cloned into BamHI/EcoRI sites of pcDNA3.1 or BglII/EcoRI sites of pEGFP(C1), and FYVE-p40^{phox}p was made using QuikChange. For PH(TAPP1)-p40^{phox} construction, two fragments (human PH domain (180–291 aa) of tandem PH domain containing protein-1 (TAPP1) (41) with BamHI/NdeI and p40^{phox}(137–341 aa) with NdeI/EcoRI) were amplified by PCR and cloned into BamHI/EcoRI sites of pcDNA3.1 or BglII/EcoRI sites of pEGFP(C1). All plasmids were sequenced to confirm their identities. Properties of p47^{phox}, p67^{phox} and p40^{phox} mutants are summarized in Table 1.

In Vitro Binding (Pull-down) Assay—The purified His$_6$-p40^{phox}(PX: 1–167 aa) protein was described previously (12). To avoid dimerization by H_2O_2, p40^{phox}(PB1: 237–339 aa) in pGEX-6P-1 (12) with a C242F mutation (GST-p40^{phox}(PB1)) was made using the QuikChange. The purified GST-p40^{phox}(PB1) and full-length His$_6$-p40^{phox} proteins were obtained as described previously (12).

The purified (His)$_6$-p40^{phox}(PX) (100 nM) was mixed with the purified GST-p40^{phox}(PB1) (100 nM) in 400 μl of the binding buffer (12). After 10 min of rotation at 4 °C, 0.01 mM H_2O_2 was added in the solution and incubated for 10 min at 4 °C. Then anti-His tag magnetic beads (MBL International) were added to the solution and rotated for 30 min at 4 °C. The precipitates were washed three times using a magnetic rack with the buffer, the material absorbed to beads was eluted in Laemmli sample buffer, and the magnetic beads were removed using a magnetic rack. The aliquots of eluants were subjected to SDS-PAGE and followed by immunoblotting using anti-GST pAb (Santa Cruz Biotechnology, Inc.; 1:1000, room temperature for 2 h). Bound antibodies were detected with secondary antibody-HRP conjugates using the ECL detection system (GE Healthcare).

The purified full-length His$_6$-p40^{phox} protein (300 nM) was mixed with biotin-coupled PI(3)P-containing polymerized liposomes (100 μM) (PI(3)P PolyPIPsomes™: Y-P003, Echelon) in 50 μl of the binding buffer (12). After 10 min of agitation at 4 °C, 0.01 mM H_2O_2 was added in the solution and incubated for 10 min at 4 °C. Then streptavidin-coupled magnetic beads (Dynabeads® M-280 Streptavidin, Invitrogen) were added to the solution and agitated for 30 min at 4 °C. The precipitates were washed three times using a magnetic rack with the buffer, the material absorbed to beads was eluted in Laemmli sample buffer, and the magnetic beads were removed using a magnetic rack. The aliquots of eluants were subjected to SDS-PAGE and followed by immunoblotting using mouse mAb against His$_6$(9C11)-peroxidase-conjugated (Wako; 1:1000 at room temperature for 2 h).

Confocal Fluorescence Imaging Studies Using Fixed Cells or Live Cells—A total of 2.5 × 10^5 cells (HEK293, HEK293$^{Nox2/Fc\gamma RIIa}$, or HEK293^{p67phox}) were seeded on 35-mm glass bottom dishes (MatTek chambers) 48 h prior to transfection and transfected using FuGENE 6. 25–30 h after the transfection, cells were fixed using 4% paraformaldehyde in HEPES buffer solution, permeabilized as described previously (37), and stained using primary Abs at room temperature for 2 h. Primary Abs were visualized by a confocal laser-scanning fluorescence microscope (LSM510 or LSM700, Zeiss) using Alexa-conjugated anti-IgG (Invitrogen; 1:2000, 0.5 h at room temperature). BIgG was prepared using 5-μm glass beads (Duke Scientific Corp.) at 10 mg/500 μl of HBSS^{++} (Invitrogen), as described previously (42). 25–30 h after the transfection, the culture medium was replaced with HBSS^{++}. After HBSS^{++} containing BIgG (five targets per cell) or H_2O_2 was added to each plate (12), images were collected at 5-s intervals for 15 min using a confocal laser-scanning fluorescence microscope with a heated stage and objective (38). The point of stimulant addition or the starting point of ingestion of added BIgG was chosen as time 0. All imaging experiments were performed in triplicate and were repeated in at least three independent transfection experiments ($n \geq 9$).

ROS Production Assay—HEK293$^{Nox2/Fc\gamma RIIa}$ and RAW246.7 cells were seeded on 6-well dishes at 2.5 × 10^5 cells/well and 1.5 × 10^5 cells/well, respectively, 48 h prior to transfection. HEK293 and RAW246.7 cells were transfected using FuGENE 6 and FuGENE HD in complexes with various combinations of plasmids, respectively. The transfection to RAW246.7 cells was most efficient by FuGENE HD among several reagents tested, and the efficacy was about 70–80% based on the imaging experiments using various GFP-based plasmids, such as GFP-p40^{phox}. The cells were fed 5 h post-transfection with complete medium and were used for assay 25–30 h after transfection. ROS release with or without stimulation (3 μl of BIgG or 200 ng/ml PMA; Sigma-Aldrich) from 2.0 × 10^5 trypsinized cells was measured by luminol-enhanced chemiluminescence methods in the presence of exogenous 10 units/ml HRP (Sigma-Aldrich) and 200 μM luminol (Sigma-Aldrich) for 20 min using a luminometer (Mithras LB940, Berthold). The ROS detected in the present study was the sum of extracellular ROS and intracellular ROS (probably including intraphagosomal ROS detected by luminol + exogenous HRP) but predominantly extracellular ROS (supplemental Fig. 1*C*). The assay (luminol-HRP without SOD + catalase; also luminol-HRP with SOD + catalase, luminol without HRP, and isoluminol-HRP) clearly shows p40^{phox} dependence in response to BIgG (supplemental Fig. 1*C*). NADPH oxidase activity was inhibited by 10 min of prior incubation with 10 μM diphenylene iodonium (Sigma-Aldrich). Comparable expression of Phox proteins was adjusted and confirmed by immunoblotting using the total lysates from the same number of cells.

Statistical Analysis—Mean oxidase activities (ROS production) were calculated from at least three independent transfection experiments and were presented as percentages (mean ± S.E.). Significant differences were calculated by Student's *t* test, and results with $p < 0.05$ were considered significant.

RESULTS

H_2O_2 Induces Conformational Changes and Targeting of p40^{phox} to Early Endosome (EE)—GFP-p40^{phox} showed a diffuse cytoplasmic localization pattern (Fig. 1*A*, *left*), whereas in sharp contrast, the PX domain of p40^{phox} was localized to dotlike, vesicular structures in resting wild type (WT) HEK293 cells (Fig. 1*A*, *center*), as reported previously in RAW 264.7 macrophages (12) and PBL-985 granulocytes (28). We (12, 27) and others (13, 31) reported that p40^{phox} mutants, such as p40^{phox}(11A:318–328), p40^{phox}(4A:318–321), p40^{phox}(F320A), p40^{phox}(E259A), and p40^{phox}(D269A), that disrupt the intermolecular PX-PB1 interaction in p40^{phox} cause a redistribution of p40^{phox} to EEs even in cells in a resting state. Consistent with those reports, p40^{phox}(F320A) showed a dot-like localization pattern in resting WT HEK293 cells (Fig. 1*A*, *right*) and moderate constitutive (32.0 ± 6.2%) or high BIgG-stimulated (371.5 ± 25.4%) ROS production when compared with control HEK293$^{Nox2/Fc\gamma RIIa}$ cells (stably expressing Nox2 and FcγRIIa; supplemental Fig. 1) transiently expressing p47^{phox} + p67^{phox} + WT p40^{phox} (Fig. 1*B*). The constitutive activity by p40^{phox}(F320A) suggests that the EE is one of the sites where ROS production occurs in HEK293$^{Nox2/Fc\gamma RIIa}$ cells, in agreement with a recent report (43). In our recent studies using RAW macrophages, we demonstrated that p40^{phox} itself or p40^{phox}-containing ternary Phox complexes translocate to EEs in response to arachidonic acid, which induces conformational changes in p40^{phox} that disrupt the intramolecular

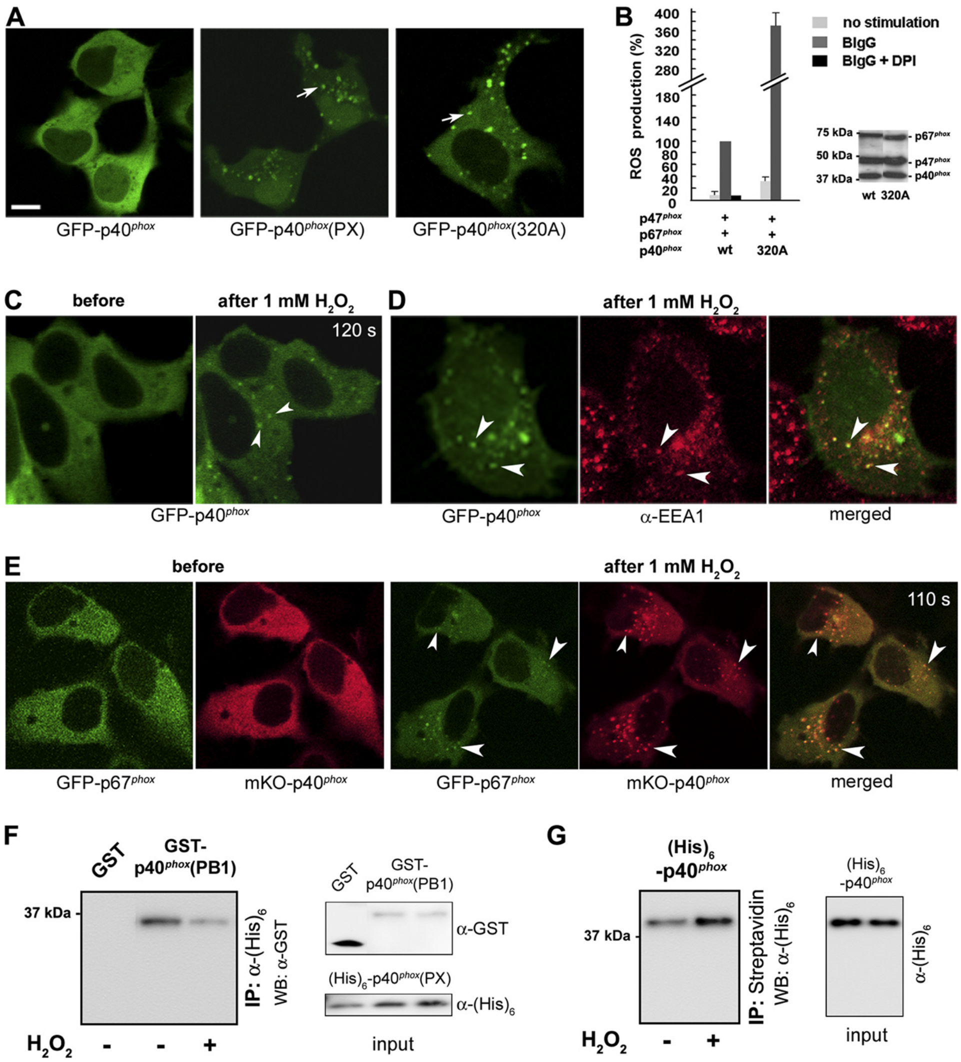

FIGURE 1. **H_2O_2 induces EE targeting of p40*^phox^*.** *A*, transfected GFP-p40*^phox^* is localized in the cytoplasm (*left*); in contrast, GFP-p40*^phox^*(PX) (*center*; *arrow*) and p40*^phox^*(F320A) (*right*; *arrow*) are localized at dotlike structures, in resting WT HEK293 cells. *Bar*, 10 μm. *B*, p40*^phox^*(F320A) co-expressed with p47*^phox^* + p67*^phox^* supports moderate constitutive (32.0 ± 6.2%) and high BIgG-stimulated ROS production in HEK293^Nox2/FcγRIIa^ cells when compared with cells expressing WT p40*^phox^* + p47*^phox^* + p67*^phox^*. Western blotting detects comparable levels of cytoplasmic Phox proteins in both transfection experiments. *C*, in response to exogenous 1 mM H_2O_2 (120 s after stimulation), GFP-p40*^phox^* expressed in WT HEK293 cells translocates to dotlike structures (*arrowheads*). *D*, the dotlike structures are co-stained by an EE marker, EEA1 (*arrowheads*). *E*, cytoplasmic GFP-p67*^phox^* co-expressed with mKO-p40*^phox^* in WT HEK293 cells translocates to dotlike structures (*arrowheads*) after stimulation (110 s) with 1 mM H_2O_2. Similar effects of H_2O_2 are observed in RAW 264.7 cells (supplemental Fig. 3). *F*, effect of H_2O_2 on the PX-PB1 domain interaction *in vitro*. The interaction between purified His_6-p40*^phox^*(PX) and GST-p40*^phox^*(PB1) proteins detected by pull-down assays is weakened by the addition of 0.01 mM H_2O_2. Similar results are obtained in three independent experiments. *G*, effect of H_2O_2 on binding of p40*^phox^* to PI(3)P *in vitro*. The interaction between purified full-length His_6-p40*^phox^* protein and PI(3)P-containing liposomes detected by pull-down assays is strengthened by the addition of 0.01 mM H_2O_2. Similar results were obtained in three independent experiments. *Error bars*, S.E.

PX-PB1 domain interaction (12). In the present study, we examined the effects of H_2O_2, which is derived from the Nox2-based NADPH oxidase and can diffuse to the cytoplasm. GFP-p40*^phox^* translocated to dotlike structures in WT HEK293 cells (Fig. 1*C*) that co-stained with EEA1 Ab, an EE marker (Fig. 1*D*), in response to 1 mM H_2O_2, whereas neither GFP-p47*^phox^* nor GFP-p67*^phox^* showed translocation to membrane structures (data not shown). Importantly, GFP-p67*^phox^* also translocated to dotlike structures when co-expressed with mKO-p40*^phox^*, which has a red fluorescent protein tag (mKO) at the N terminus, after stimulation with H_2O_2 both in WT HEK293 cells (Fig. 1*E*) and in RAW macrophages (supplemental Fig. 3). Furthermore, inhibition of PI(3)P production on EEs by a PI 3-kinase inhibitor, wortmannin (100 nM for 15 min), showed no dotlike localization of GFP-p40*^phox^*(PX) or translocation of GFP-p40*^phox^* to dotlike structures in response to H_2O_2 in RAW macrophages (supplemental Fig. 4).

These results suggest that H_2O_2 induces conformational changes within p40*^phox^* in the cytoplasm, enabling it to function as a carrier protein that directs the cytoplasmic Phox complex to PI(3)P-enriched membranes. To support this speculation, we performed a binding (pull-down) experiment using purified His_6-p40*^phox^*(PX) and GST-p40*^phox^*(PB1) proteins. H_2O_2 (0.01 mM) weakened the interaction between His_6-p40*^phox^*(PX) and GST-p40*^phox^*(PB1), further suggesting that H_2O_2 induces some conformational changes in the PX and/or the PB1 domain of p40*^phox^* (Fig. 1*F*). Furthermore, in an *in vitro* binding assay using purified full-length His_6-p40*^phox^* protein and PI(3)P-containing liposomes, H_2O_2 (0.01 mM) strengthened the interaction between His_6-p40*^phox^* and PI(3)P, suggesting that H_2O_2 induces

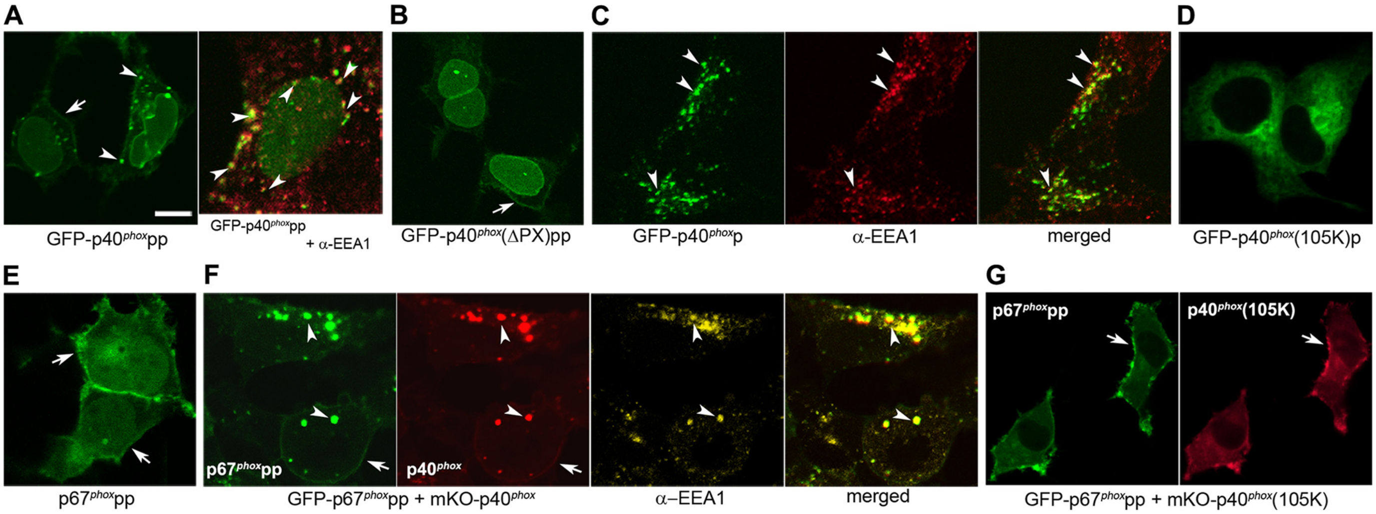

FIGURE 2. **Direct or indirect membrane targeting of $p40^{phox}$ induces EE-targeting of $p40^{phox}$ in WT HEK293 cells.** *A*, transfected GFP-$p40^{phox}$pp is localized at dotlike structures (*left*; *arrowheads*) in addition to PM (*left*; *arrow*). The dotlike structures are co-stained with EEA1 (*right*; *arrowheads*). *Bar*, 10 μm. *B*, the dotlike localization of GFP-$p40^{phox}$pp disappears in the case of GFP-$p40^{phox}$(ΔPX)pp. *Arrow*, PM. *C*, GFP-$p40^{phox}$p is co-stained with EEA1 (*arrowheads*). A movie of accumulation on phagosome of $p40^{phox}$p during ingestion of BIgG in $HEK293^{Nox2/Fc\gamma RIIa}$ cells is available (supplemental Video 1). *D*, the dotlike localization of GFP-$p40^{phox}$p disappears in the case of GFP-$p40^{phox}$(R105K)p. *E*, PM-targeting mutant of cytoplasmic GFP-$p67^{phox}$, GFP-$p67^{phox}$pp, shows PM localization (*arrows*) in addition to nuclear localization. *F*, when cytoplasmic mKO-$p40^{phox}$ is co-expressed with GFP-$p67^{phox}$pp, both proteins are co-localized at EEs stained by EEA1 (using Cy5-conjugated secondary Ab) (*arrowheads*) in addition to the PM (*arrow*). *G*, the dotlike localization of both proteins disappears in the case of mKO-$p40^{phox}$(R105K) + GFP-$p67^{phox}$pp. *Arrow*, PM.

disruption of the PX-PB1 domain interaction within $p40^{phox}$ (Fig. 1*G*).

Direct or Indirect Membrane Targeting of $p40^{phox}$ Induces Recruitment of $p40^{phox}$ to EE—To examine the possibility that $p40^{phox}$ also develops PI(3)P-binding capabilities after membrane targeting, we utilized a PM-targeting motif consisting of the polybasic and prenylated (pp) C-terminal sequence of Rac1 (183–192 aa; KKRKRKCLLL) or the intracellular endomembrane-targeting prenylated (p) motif (189–192 aa; CLLL) of Rac1 fused onto GFP-tagged $p40^{phox}$, according to previous reports (36, 37, 44–46). GFP-$p40^{phox}$pp was localized at EEs in addition to the PM (Fig. 2*A*), and this EE localization pattern was abolished with GFP-$p40^{phox}$(ΔPX)pp, lacking the PX domain in WT HEK293 cells (Fig. 2*B*). GFP-$p40^{phox}$p was also targeted to EEA1-positive dotlike structures both in WT HEK293 (Fig. 2*C*) and $HEK293^{Nox2/Fc\gamma RIIa}$ cells (supplemental Video 1), and this EE localization was abolished in the case of the PX domain mutant (Fig. 2*D*), GFP-$p40^{phox}$(R105K)p, which loses its capabilities to bind PI(3)P.

To further investigate the possibility that indirect membrane targeting of $p40^{phox}$ also induces conformational changes in $p40^{phox}$ promoting its binding to PI(3)P, we used a PM-targeted mutant of $p67^{phox}$, GFP-$p67^{phox}$pp. GFP-$p67^{phox}$ is a cytoplasmic protein in resting cells (12); however, GFP-$p67^{phox}$pp showed PM localization in WT HEK293 cells (Fig. 2*E*). When cytoplasmic mKO-$p40^{phox}$ was co-expressed with GFP-$p67^{phox}$pp, mKO-$p40^{phox}$ and GFP-$p67^{phox}$pp co-localized at EEs in addition to the PM in WT HEK 293 cells (Fig. 2*F*). This EE but not PM localization of mKO-$p40^{phox}$ was abolished in the case of mKO-$p40^{phox}$(R105K), which does not bind PI(3)P (39) (Fig. 2*G*).

These results suggest that PM or endomembrane targeting of $p40^{phox}$, whether through direct or indirect means, caused recruitment of $p40^{phox}$ to PI(3)P-enriched EEs through subcellular membrane cycling (PM to EEs in the endocytic pathway (47, 48) and endomembranes to EEs in the retrograde-transport and anterograde-transport pathways (49)); finally, $p40^{phox}$ bound to PI(3)P and accumulated on the membranes of EE. In agreement with our data, a recent study reported that the membrane-spanning Phox protein (heterodimer of Nox2 and $p22^{phox}$) was localized on the recycling endosomes as well as EEs and PM in CHO model cells and macrophages (43). Thus, $p40^{phox}$ probably develops PI(3)P-binding capabilities also through direct or indirect membrane targeting and may even promote these membrane cycling and trafficking pathways through PI(3)P binding.

Indirect Membrane Targeting of $p40^{phox}$ through $p47^{phox}$-$p67^{phox}$-$p40^{phox}$ Interaction Induces Recruitment of $p40^{phox}$ to EE—$p47^{phox}$ functions as a carrier and adaptor protein of the cytoplasmic ternary Phox complex (5, 21, 33, 50). We first examined the possibility that indirect membrane targeting of $p40^{phox}$ as a component of the ternary $p47^{phox}$-$p67^{phox}$-$p40^{phox}$ complex induces conformational changes within $p40^{phox}$ that enable it to bind to PI(3)P and localize at PI(3)P-enriched membranes. When GFP-$p47^{phox}$ and mKO-$p40^{phox}$ were co-expressed in $HEK293^{p67phox}$ cells (stably expressing $p67^{phox}$; supplemental Fig. 5*A*), both were localized in the cytoplasm (Fig. 3*A*). Intriguingly, when cytoplasmic mKO-$p40^{phox}$ was co-expressed with an intracellular endomembrane-targeted mutant of GFP-$p47^{phox}$, GFP-$p47^{phox}$p (Fig. 3*B*), dotlike structures containing GFP-$p47^{phox}$p, mKO-$p40^{phox}$, and $p67^{phox}$ appeared (Fig. 3*C* and supplemental Fig. 5*B*) in $HEK293^{p67phox}$ cells, which were not observed in the case of mKO-$p40^{phox}$(R105K) (Fig. 3*D*). To explore an alternative means for indirect $p40^{phox}$ membrane targeting through the $p47^{phox}$-$p67^{phox}$-$p40^{phox}$ interaction, a PM-targeted mutant of $p47^{phox}$ was used in which its PX domain was replaced with that of Noxo1, which constitutively localizes at the PM even in resting cells (40, 51). When

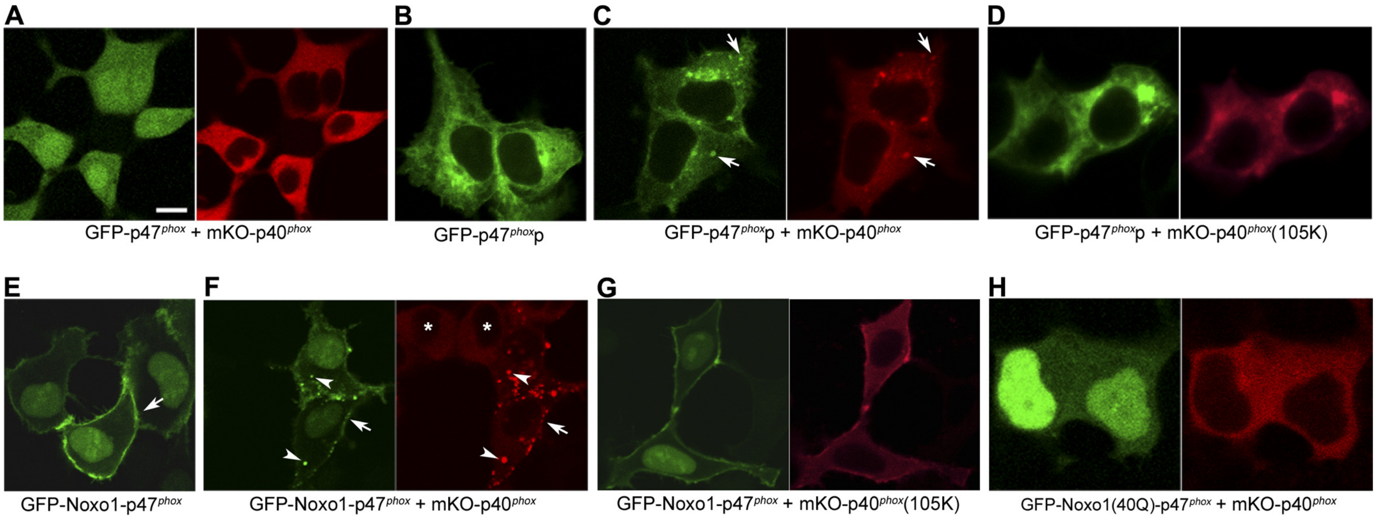

FIGURE 3. **Indirect membrane targeting of p40^{phox}by p47^{phox}p or Noxo1-p47^{phox} through the p47^{phox}-p67^{phox}-p40^{phox} interaction induces EE localization of p40^{phox} in HEK293^{p67phox} cells.** *A*, both GFP-p47^{phox} and mKO-p40^{phox} are localized in the cytoplasm. *Bar*, 10 μm. *B*, GFP-p47^{phox}p has a reticular, nuclear membrane and Golgi complex localization. *C*, in the case of co-expression of GFP-p47^{phox}p and mKO-p40^{phox}, dotlike structures with GFP-p47^{phox}p and mKO-p40^{phox} appear (*arrows*). Co-staining of stably expressed p67^{phox} at the dotlike structures is shown in supplemental Fig. 5*B*. *D*, the dotlike structures disappear in the case of co-expression of GFP-p47^{phox}p and mKO-p40^{phox}(R105K). *E*, GFP-Noxo1-p47^{phox} shows PM localization (*arrow*) in addition to nuclear localization. *F*, with co-expression of GFP-Noxo1-p47^{phox} and mKO-p40^{phox}, mKO-p40^{phox} is localized at dotlike structures (*arrowheads*) in addition to PM (*arrow*) with GFP-Noxo1-p47^{phox}. In contrast, without co-expression of GFP-Noxo1-p47^{phox}, mKO-p40^{phox} is localized in the cytoplasm (*asterisks*). *G*, the dotlike localization, but not PM localization, of both proteins disappears in the case of co-expression of GFP-Noxo1-p47^{phox} and mKO-p40^{phox}(R105K). *H*, both the dotlike and PM localizations of both proteins disappear with co-expression of GFP-Noxo1(R40Q)-p47^{phox} and mKO-p40^{phox}.

mKO-p40^{phox} was co-expressed with GFP-Noxo1-p47^{phox} in HEK293^{p67phox} cells (Fig. 3*E*), mKO-p40^{phox} also showed a dotlike localization pattern, in addition to PM localization with GFP-Noxo1-p47^{phox} (Fig. 3*F*). These dotlike structures were co-stained with EEA1 (data not shown). The dotlike localization, but not PM localization, of GFP-Noxo1-p47^{phox} and mKO-p40^{phox} disappeared in the case of mKO-p40^{phox}(R105K) (Fig. 3*G*). GFP-Noxo1(R40Q)-p47^{phox}, which loses its PM-targeting capabilities by mutation in the PX domain (40), showed no dotlike or PM localization with mKO-p40^{phox} (Fig. 3*H*). Furthermore, neither the dotlike nor PM localizations of mKO-p40^{phox} were observed in WT HEK293 cells when GFP-Noxo1-p47^{phox} was co-expressed with p67^{phox}(K355A), which disrupts interaction between p67^{phox} and p40^{phox} (supplemental Fig. 5*C*).

These data show that indirect targeting of p40^{phox} to membranes through other Phox protein interactions enables p40^{phox} to bind to PI(3)P, thereby redirecting the cytoplasmic ternary Phox complex to PI(3)P-enriched membranes.

The p40^{phox} High Affinity PI(3)P-binding PX Domain Is Critical for BIgG-stimulated Nox2 Activation—To examine the importance of PI(3)P binding to p40^{phox} in Nox2 activation, we substituted its PX domain with other PI(3)P-specific binding domains, the FYVE domain from Hrs in addition to the PI(3,4)P_2-specific PH domain from TAPP1 and the PI(3,4,5)P_3-specific PH domain from GRP1 (general receptor for phosphoinositides-1), which were expressed in HEK293$^{Nox2/Fc\gamma RIIa}$ cells. GFP-FYVE showed no accumulation on phagosomes (data not shown), as described previously (52). In contrast, GFP-2xFYVE, which has about a 10-fold higher affinity for PI(3)P than GFP-FYVE (53), was localized at EE and accumulated on phagosomes by fusion with EE during ingestion of BIgG (data not shown), as observed with the p40^{phox} PX domain (12), indicating that a threshold affinity for PI(3)P drives this translocation. GFP-PH(TAPP1) and GFP-PH(GRP1), which are primarily localized in the cytoplasm, also showed accumulation on phagosomes (data not shown). We then made chimeric mutants of p40^{phox} replacing the PX domain with the FYVE, PH(TAPP1), or PH(GRP1) domains (FYVE-p40^{phox}, PH(TAPP1)-p40^{phox}, or PH(GRP1)-p40^{phox}). It is unlikely that the FYVE or PH domains in these chimeric proteins are masked by the PB1 domain of p40^{phox}, because the three-dimensional structures of these domains are quite different from that of the PX domain of p40^{phox} (54, 55). Weak accumulation of GFP-p40^{phox} on phagosomes was sometimes observed in HEK293$^{Nox2/Fc\gamma RIIa}$ cells without co-expression of p47^{phox} or p67^{phox} (Fig. 4*A* and supplemental Video 2), consistent with our previous report (12). The PX domain of p40^{phox} has a high affinity for PI(3)P (K_d to 0.5% PI(3)P lysosome: 40 $\pm$ 7 nM (56)) but is masked by the PB1 domain. Accumulation of GFP-FYVE-p40^{phox}, which has a low affinity domain (FYVE) for PI(3)P (K_d to 0.5% PI(3)P lysosome: 420 $\pm$ 8 nM (57); more than 10 times lower affinity than that of PX domain of p40^{phox} (58)) but is not masked by the PB1 domain, was never observed (Fig. 4*B* and supplemental Video 3). In contrast, GFP-PH(TAPP1)-p40^{phox} (Fig. 4*C* and supplemental Video 4) and GFP-PH(GRP1)-p40^{phox} (data not shown), containing PH domains with a high affinity for PI(3,4)P_2 (K_d of TAPP1 to 0.5% PI(3,4) P_2 lysosome: 1.5 $\pm$ 0.5 nM (18); K_d of TAPP1 to PI(3,4)P_2: 40.1 nM (41)) and for PI(3,4,5)P_3 (K_d of GRP1 to PI(3,4,5)P_3: 59.2 nM (41)), respectively, were readily detected on nascent phagosomes. A membrane-targeted mutant of FYVE-p40^{phox}, FYVE-p40^{phox}p, showed EE localization (Fig. 4*D*) and accumulated on phagosomes by fusion of EE during ingestion of BIgG. (supplemental Video 5). From the standpoint of ROS production, PH(TAPP1)-p40^{phox} showed about 4-fold higher ROS production compared with p40^{phox},

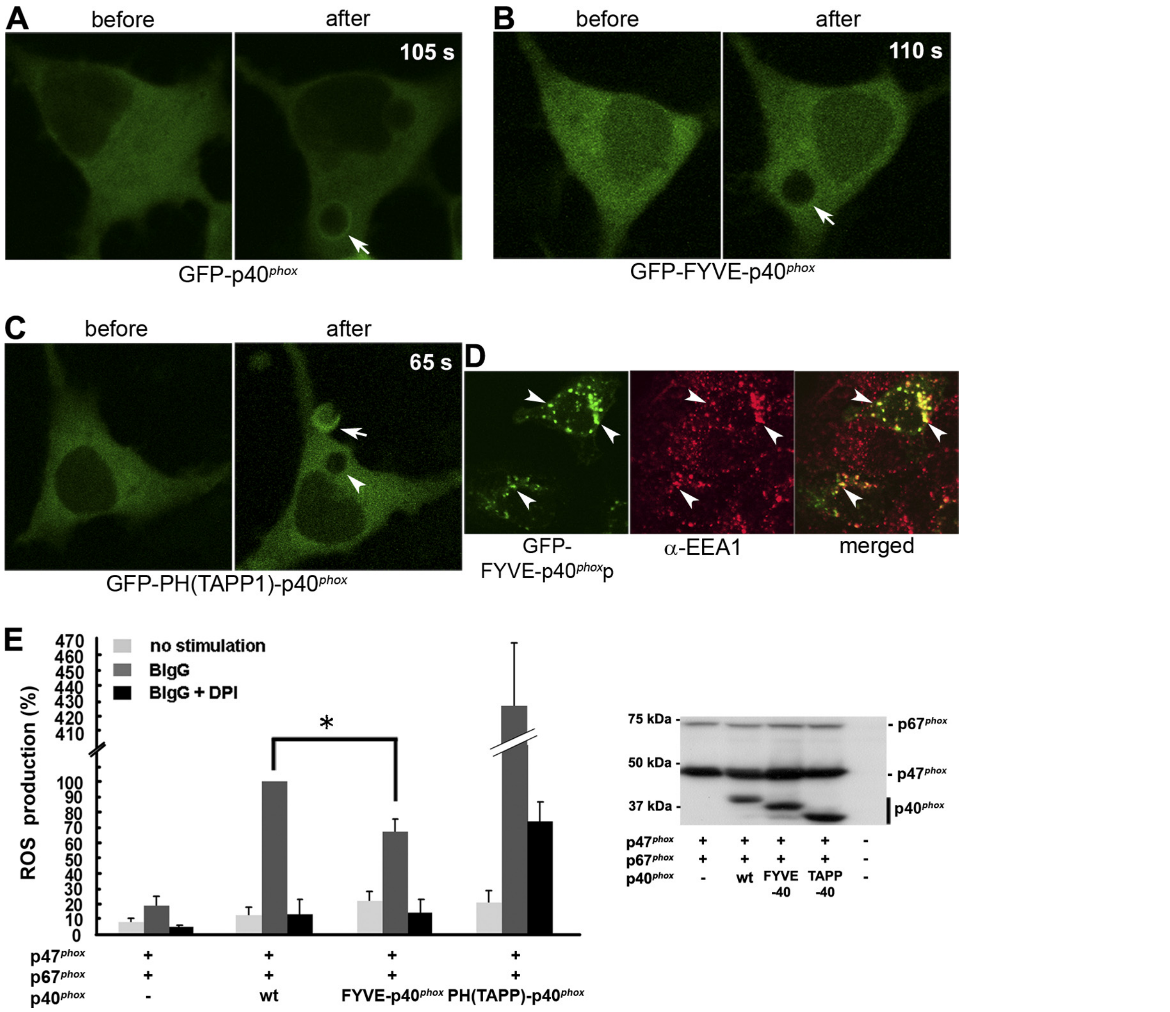

FIGURE 4. **High affinity PI(3)P-binding PX domain is a critical determinant of p40^{phox} phagosomal accumulation and oxidase function in HEK293$^{Nox2/Fc\gamma RIIa}$ cells.** *A*, weak accumulation of GFP-p40^{phox} on phagosome 105 s after the start of BIgG ingestion is shown (*arrow*). A movie is available (supplemental Video 2). *B*, no accumulation of GFP-FYVE-p40^{phox} on phagosome is observed (*arrow*). A movie is available (supplemental Video 3). *C*, accumulation of GFP-PH(TAPP1)-p40^{phox} on nascent phagosomal cup is observed 65 s after starting BIgG ingestion (*arrow*). No accumulation of GFP-PH(TAPP1)-p40^{phox} on mature phagosome is observed (*arrowhead*). A movie is available (supplemental Video 4). *D*, FYVE-p40^{phox}p is localized at dotlike structures that co-stained with EEA1 (*arrowheads*). A movie of accumulation on phagosome of FYVE-p40^{phox}p during ingestion of BIgG is available (supplemental Video 5). *E*, BIgG-stimulated ROS production is enhanced 4-fold by p47^{phox} + p67^{phox} + PH(TAPP1)-p40^{phox} and is statistically decreased by p47^{phox} + p67^{phox} + FYVE-p40^{phox} when compared with p47^{phox} + p67^{phox} + p40^{phox}. *, $p < 0.05$. *Error bars*, S.E.

whereas FYVE-p40^{phox} showed statistically lower ROS production than p40^{phox} (67.4 ± 9.6%) (Fig. 4*E*). Comparable expression of p47^{phox}, p67^{phox}, p40^{phox}, and p40^{phox} chimeric mutants was confirmed by immunoblotting (Fig. 4*E*).

These results indicate that the high affinity of the PX domain of p40^{phox} for PI(3)P, even when masked by the PB1 domain in the resting state, initiates or dictates its accumulation on phagosomes. Despite the limitations of FYVE-p40^{phox} detection by imaging these fluorescent-tagged proteins, even the basal level affinity for PI(3)P binding of the PX domain of p40^{phox} or FYVE domain appears to influence ROS production.

The Phosphorylation Status of p47^{phox} Influences the Dependence of Nox2-ROS Production on PI(3)P Binding by p40^{phox}—To further examine the consequences of indirect membrane targeting of p40^{phox} through its interactions with p47^{phox} and p67^{phox}, we used a mutant, p47^{phox}(ΔAIR), in which the autoinhibitory region (AIR) is deleted. p47^{phox}(ΔAIR) renders p47^{phox} constitutively active and capable of membrane binding, supporting Nox2-based ROS production without stimulation because of its constitutive interaction with p22^{phox} in resting cells (59). ROS production using p47^{phox}(ΔAIR) HEK293$^{Nox2/Fc\gamma RIIa}$ cells was constitutive, was only slightly enhanced by BIgG stimulation, and was effectively inhibited by diphenylene iodonium (Fig. 5*A*). Enhanced ROS production by the addition of p40^{phox} to p47^{phox}(ΔAIR) + p67^{phox} was probably due to enhanced stabilization of p67^{phox} protein levels by p40^{phox} (Fig. 5*A*). Most importantly, ROS production by p47^{phox}(ΔAIR) + p67^{phox} + p40^{phox} was independent of the PI(3)P-binding capabilities of p40^{phox} (Fig. 5*A*). Comparable expression levels of proteins were confirmed by immunoblotting (Fig. 5*A*). These results indicate that deletion of the AIR of p47^{phox} leads to constitutive binding to p22^{phox}, thereby inducing constitutive oxidase activity and only minor enhancing effects of BIgG, which are independent of the PI(3)P-binding capabilities of p40^{phox}. To investigate the relationship between the phosphorylation status of p47^{phox} and the dependence on p40^{phox}-PI(3)P binding for ROS production by the Nox2-based oxidase, we used seven phosphorylation site-mimicking mutants of p47^{phox}. ROS produc-

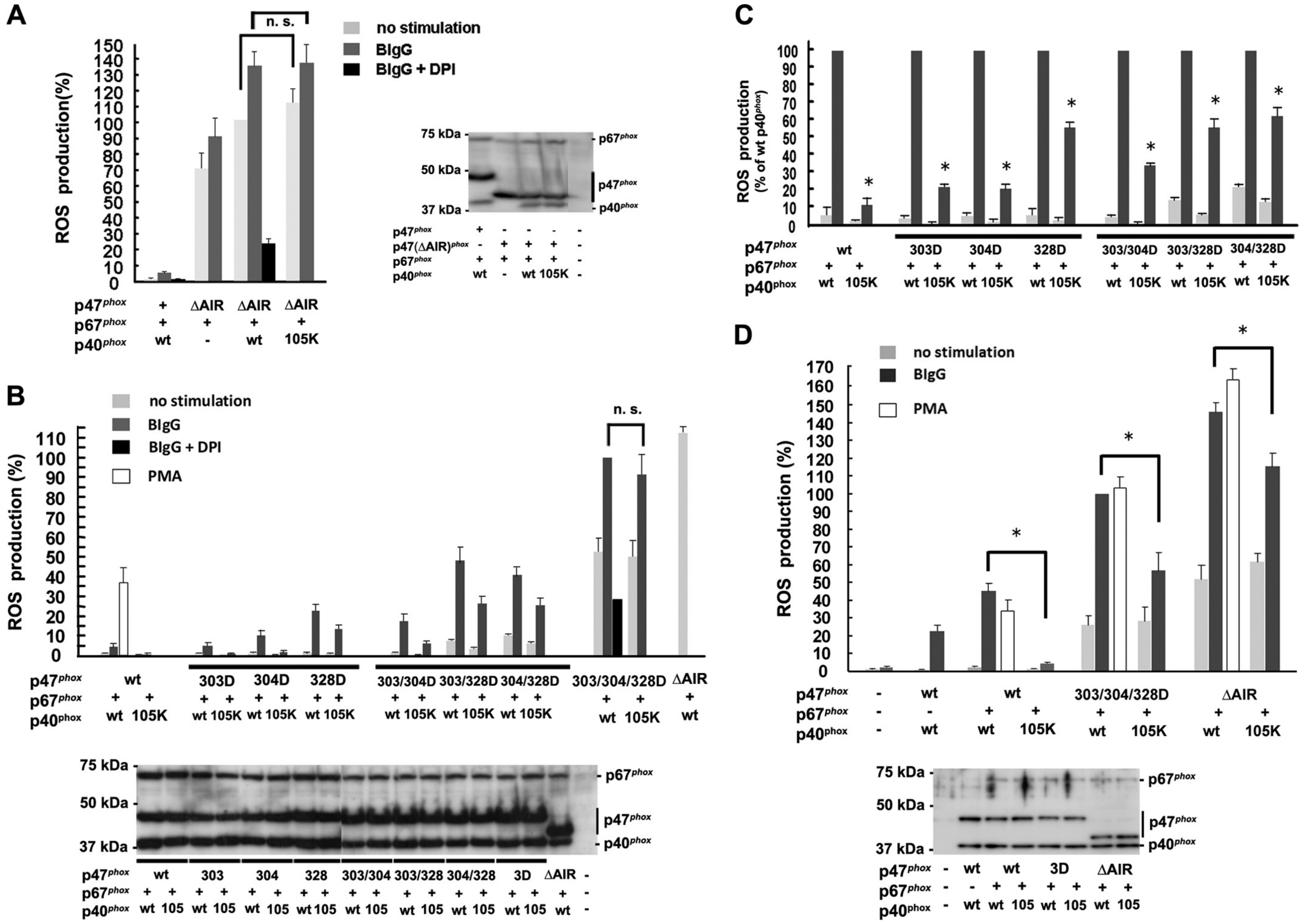

FIGURE 5. **Dependence of PI(3)P-binding of p40*phox* in ROS production by Nox2 is determined by the phosphorylation status of p47*phox* in both HEK293$^{Nox2/Fc\gamma RIIa}$ (*A–C*) and RAW264.7$^{p40/p47KD}$ cells (*D*).** *A*, ROS production using p47*phox*(ΔAIR) is constitutive, shows small BIgG dependence, and is effectively inhibited by 10 μM diphenylene iodonium. The addition of p40*phox* enhances ROS production by p47*phox*(ΔAIR) and p67*phox*. ROS production by p47*phox*(ΔAIR) + p67*phox* + p40*phox* is independent of the PI(3)P-binding capabilities of p40*phox* (p40*phox*(R105K)). *n.s.*, not statistically significant. *B*, ROS production using one- or two-site phosphorylation-mimicking mutants of p47*phox* as well as WT p47*phox* shows PI(3)P-binding of p40*phox* dependence; however, p47*phox*(S303D/S304D/S328D) is independent of PI(3)P binding to p40*phox*. All mimicking mutants showed higher ROS production than WT p47*phox*. *3D*, S303D/S304D/S328D. *C*, PI(3)P dependence in ROS production using WT or one- or two-site phosphorylation-mimicking mutants of p47*phox*. Data shown in *B* are normalized to activities supported by WT p40*phox*. All mimicking mutants show less PI(3)P dependence than WT p47*phox*. The mimicking mutants having Asp-328 (S328D, S303D/S328D, and S304D/S328D) show constitutive activity without BIgG and less PI(3)P dependence than S303D, S304D, or S303D/S304D. *, $p < 0.01$. *D*, in RAW264.7$^{p40/p47KD}$ cells, ROS production using WT p47*phox* shows almost complete dependence on PI(3)P binding to p40*phox*. In contrast, reconstituted ROS production by p47*phox*(S303D/S304D/S328D) or p47*phox*(ΔAIR) shows only moderate PI(3)P dependence. *, $p < 0.01$. *3D*, S303D/S304D/S328D. *Error bars*, S.E.

tion using p47*phox*(S303D/S304D/S328D), which is a phosphorylation-mimicking mutant of p47*phox* sufficient for access to p22*phox* without cell stimulation (60), was not affected by the R105K mutation of p40*phox* in HEK293$^{Nox2/Fc\gamma RIIa}$ cells and was therefore independent of PI(3)P binding (Fig. 5*B*), as in the case of p47*phox*(ΔAIR). However, ROS production in response to BIgG using one or two phosphorylation site-mimicking mutants of p47*phox* (S303D, S304D, S328D, S303D/S304D, S303D/S328D, or S304D/S328D) was dependent on p40*phox* PI(3)P binding (Fig. 5*B*), and all of the phosphorylation-mimicking mutants showed higher ROS production (Fig. 5*B*) and less PI(3)P dependence than in the case of WT p47*phox* (Fig. 5*C*). Interestingly, the mimicking mutants having S328D (S328D, S303D/S328D, and S304D/S328D) showed constitutive activity without BIgG stimulation, higher ROS production, and less PI(3)P dependence than in the case of S303D, S304D, or S303D/S304D (Fig. 5*C*). PI(3)P binding independence in p47*phox*(S303D/S304D/S328D) and p47*phox*(ΔAIR), but not in two-site phosphorylation-mimicking mutants of p47*phox* (S303D/S304D, S303D/S328D, and S304D/S328D), was also detected by a ROS production assay using luminol without exogenous HRP (supplemental Fig. 6). Phosphorylation of WT p47*phox* in response to BIgG in HEK293$^{Nox2/Fc\gamma RIIa}$ cells was confirmed using ^{32}P label (supplemental Fig. 7). Comparable expression of p47*phox*, p47*phox* mutants, p67*phox*, p40*phox*, and p40*phox*(R105K) was confirmed by immunoblotting (Fig. 5*B*). Taken together, it appears that the dependence on p40*phox* PI(3)P binding for ROS production by Nox2 is determined by the phosphorylation status of p47*phox*, which governs the interaction between p47*phox* and p22*phox*; complete constitutive (high affinity) interaction with p22*phox* results in maximum ROS production with PI(3)P independence, whereas incom-

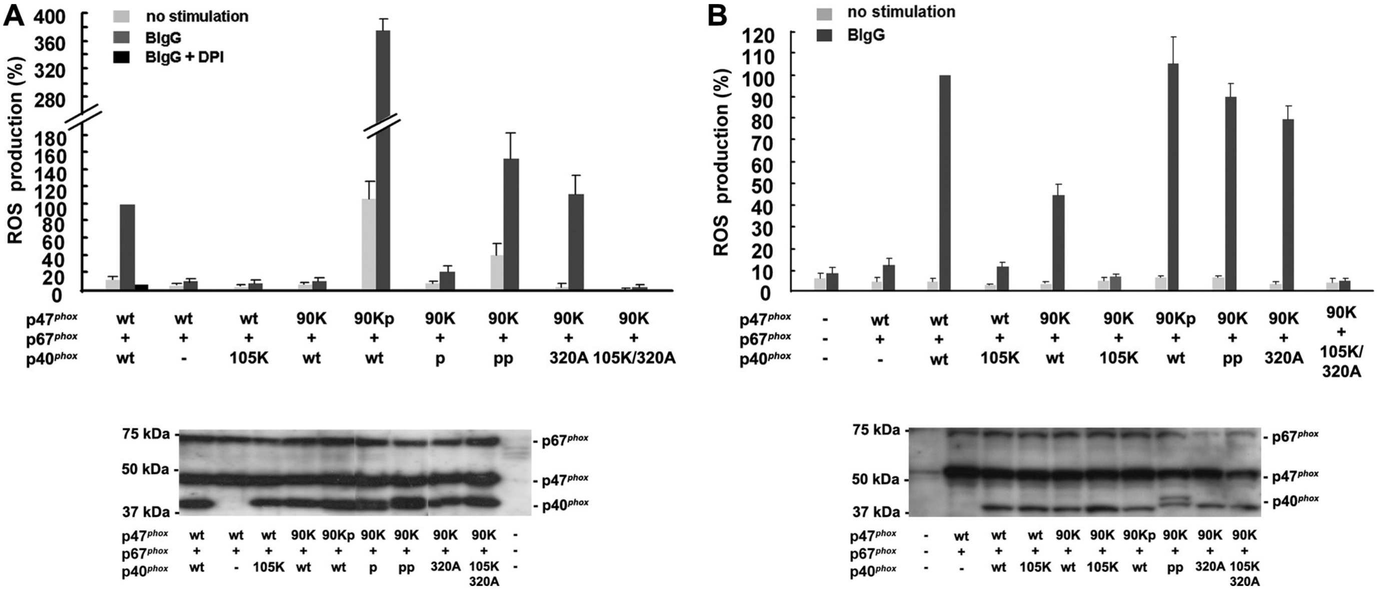

FIGURE 6. **Membrane-associating mutants of p40^{phox} can rescue the function of the PX domain of p47^{phox}.** *A*, in HEK293$^{Nox2/Fc\gamma RIIa}$ cells, ROS production by p47^{phox}(R90K) + p67^{phox} + p40^{phox} is almost absent, whereas p47^{phox}(R90K)p dramatically rescues reconstituted ROS production. p40^{phox}pp, but not p40^{phox}p, is able to completely rescue ROS production by p47^{phox}(R90K) + p67^{phox} + p40^{phox}. p40^{phox}(F320A), which is targeted to EE by disrupted PX-PB1 intermolecular interaction (Fig. 1*A*), effectively rescues ROS production by p47^{phox}(R90K) + p67^{phox} + p40^{phox}, whereas p40^{phox}(R105K/F320A) does not. *B*, in RAW264.7$^{p40/p47KD}$ cells, WT p40^{phox}, but not p40^{phox}(R105K), moderately rescues ROS production with p47^{phox}(R90K). Membrane-associating mutants, p47^{phox}(R90K)p, p40^{phox}pp, and p40^{phox}(F320A) almost completely rescue reconstituted ROS production with p47^{phox}(R90K). *Error bars*, S.E.

plete (low affinity) interaction with p22^{phox} favors PI(3)P dependence involving p40^{phox}.

These results were confirmed in similar experiments using RAW264.7$^{P40/p47KD}$ cells (stable knockdown of both p40^{phox} and p47^{phox}; supplemental Fig. 2). Although PI(3)P dependence was still seen in reconstituted ROS production with p47^{phox}(S303D/S304D/S328D) or p47^{phox}(ΔAIR) (Fig. 5*D*), the order of PI(3)P dependence was WT p47^{phox} $\gg$ p47^{phox}(S303D/S304D/S328D) $>$ p47^{phox}(ΔAIR) in three different assays (Fig. 5*D* and supplemental Fig. 8, *A* and *B*). Comparable expression of p47^{phox}, p47^{phox} mutants, p67^{phox}, p40^{phox}, and p40^{phox}(R105K) was confirmed by immunoblotting (Fig. 5*D*).

Membrane-associating Mutants of p40^{phox} Can Rescue the PI-binding Function of the PX Domain of p47^{phox}—Finally, to examine the contribution of the adaptor functions of p40^{phox} in the Nox2-based oxidase, we used membrane-targeted mutants of p40^{phox} and p47^{phox}(R90K), which is a PI binding-deficient (50, 61) and membrane targeting-defective mutant protein (12, 18, 56). ROS production reconstituted by p47^{phox}(R90K) + p67^{phox} + p40^{phoxv} was significantly decreased in HEK293$^{Nox2/Fc\gamma RIIa}$ cells, consistent with previous studies (50) (Fig. 6*A*); however, ROS production was dramatically rescued by the membrane-targeted version of p47^{phox}(R90K), p47^{phox}(R90K)p (Fig. 6*A*). Although p40^{phox}p rescued some ROS production by p47^{phox}(R90K) + p67^{phox} + p40^{phox}, considerably higher ROS production was rescued using p40^{phox}pp (Fig. 6*A*). Intriguingly, p40^{phox}(F320A), which is a mutant freely accessible to PI(3)P with a disrupted intermolecular PX-PB1 interaction, fully rescued ROS production by p47^{phox}(R90K) + p67^{phox} + p40^{phox}, whereas p40^{phox}(R105K/F320A) supported no activity (Fig. 6*A*). Comparable expression of p47^{phox}, p47^{phox} mutants, p67^{phox}, p40^{phox}, and p40^{phox} mutants was confirmed by immunoblotting (Fig. 6*A*). These findings complement observations on ROS production using p47^{phox}(ΔAIR) or p47^{phox}(S303D/S304D/S328D), which were not affected by the R105K mutation in p40^{phox} (Fig. 5, *A* and *B*), and suggest that strong membrane associations in p40^{phox}, seen in p40^{phox}pp or p40^{phox}(F320A), could restore ROS production in the absence of PI binding to p47^{phox} in HEK293$^{Nox2/Fc\gamma RIIa}$ cells.

These results were confirmed in similar experiments using RAW264.7$^{P40/p47KD}$ cells in which WT p40^{phox}, but not p40^{phox}(R105K), showed moderate restoring capabilities in reconstituted ROS production by p47^{phox}(R90K) (Fig. 6*B*). Comparable expression of p47^{phox}, p47^{phox} mutants, p67^{phox}, p40^{phox}, and p40^{phox} mutants was confirmed by immunoblotting (Fig. 6*B*).

DISCUSSION

It has been well recognized that p47^{phox} serves as a carrier of the cytoplasmic ternary Phox complex to membranes, using its PX domain, and also serves as an adaptor between the cytoplasmic Phox complex and the membrane-spanning flavocytochrome b_{558}; thus, p47^{phox} is called as an "organizer" of the Nox2 complex (2, 3). Although we and others reported that p40^{phox} also acts as a carrier of the ternary Phox complex during FcγR-mediated (12, 27), PMA-stimulated (29–31), and fMLP-stimulated oxidative bursts (30), another report suggests that p40^{phox} primarily functions in Nox2 activation on phagosomes (32). We showed here that the dependence on p40^{phox} PI(3)P binding for Nox2 activity is determined, at least partly, by the phosphorylation status of p47^{phox}. p40^{phox} is essential during FcγR-mediated oxidase activation; however, p40^{phox} is less critical under conditions when p47^{phox} is adequately phosphorylated and binds to p22^{phox} efficiently, as revealed when examining phosphorylation/activation-mimicking p47^{phox} mutants (*i.e.* p47^{phox}(ΔAIR) and p47^{phox}(S303D/S304D/S328D)) (Fig. 5 and supplemental Figs. 6 and 8). In the present study, we showed the dependence on p40^{phox} PI(3)P binding for Nox2 activity (both for extracellular and intracellular ROS) during FcγR-mediated oxidative burst, based on the following methods and observations: 1) in assays using luminol with HRP (measuring total ROS but predominantly extracellular ROS), in assays using luminol with HRP + (SOD + catalase) (measuring intracellular ROS), in assays using luminol without HRP (measuring intracellular ROS), or in assays using isoluminol with HRP (measuring extracellular ROS) in HEK293$^{Nox2/Fc\gamma RIIa}$ cells (Fig. 5, *A* and *B*, and supplemental Figs. 1 and 6); 2) in assays using RAW264.7$^{P40/p47KD}$ cells (Fig. 5*D* and supplemental Fig. 8); and 3) based on a report demonstrating p40^{phox} and PI(3)P binding dependence during FcγR-mediated oxidative burst (measured using luminol with HRP) in COS7 cells stably expressing Phox proteins and FcγRIIa (32). A series of stepwise phosphorylation events at eight distinct phosphorylated sites within p47^{phox} were reported (8, 9), of which only four are prominently phosphorylated in membrane-bound p47^{phox} fractions in early phases of stimulation in normal neutrophils but not in flavocytochrome b_{558}-deficient CGD neutrophils (8). We demonstrated that PI binding (*i.e.* membrane targeting) (12, 18, 56), by p47^{phox} is less critical (Fig. 6) when the autoinhibitory (PX-PB1) interaction within p40^{phox} is released and allows binding to PI(3)P or when p40^{phox} is targeted to membranes by other means, as seen with p40^{phox}(F320A) and p40^{phox}pp. These observations strongly support the proposed carrier function of p40^{phox} in delivering the ternary Phox complex to phagosomes in cooperation with p47^{phox} under conditions when p47^{phox} is only partially phosphorylated (*e.g.* in the initial stages of translocation of the Phox complex to phagosomes) or when PI levels are insufficient to bind p47^{phox} (*e.g.* in late stages of phagocytosis) (12). Furthermore, although the function of p40^{phox} as a carrier and adaptor seems to be less prominent than p47^{phox} (Fig. 6*A*), we propose that both p40^{phox} and p47^{phox} are required for orchestrating optimal phagosome-targeting of the cytoplasmic Phox complex and also for stable assembly and retention of the Nox2 complex on phagosomes during the FcγR-mediated oxidative burst. Several reports support this concept of a functional partnership of both proteins: p47^{phox} is required for phagosome-targeting of p67^{phox} and ROS production in p47^{phox}-deficient neutrophils (23); p40^{phox}-deficient neutrophils exhibit a severe defect in FcγR-mediated oxidative burst but not in PMA- or fMLP-stimulated ROS production (28); PI(3)P-binding capabilities of p40^{phox} are required for prolonged retention of p40^{phox} (28) and the p40^{phox}-p67^{phox}-p47^{phox} complex (27) on phagosomes; autosomal recessive CGD patients, including a p40^{phox}-deficient patient, suffer less severe clinical phenotypes than X-linked CGD patients (62); phosphorylation of p40^{phox} on Thr-154 is required for phagosome targeting of p47^{phox} and ROS production in reconstituting p40^{phox}-deficient (or knockdown) neutrophils (63); and both p40^{phox} and p47^{phox} are required for ROS production in microvascular endothelial cells (64).

It was reported that translocation of p67^{phox}, involving the carrier function of p40^{phox}, is dependent on the PX domain of p40^{phox} but is PI(3)P-independent and that activation of Nox2 is PI(3)P-dependent in PMA-stimulated, permeabilized PLB-985 neutrophil cores (31). These authors speculated that moesin (65), a cytoskeletal protein, instead of PI(3)P may be a predominant target of the p40^{phox} PX domain in the PMA-stimulated oxidative burst of permeabilized cores (31). In the present study using HEK293$^{Nox2/Fc\gamma RIIa}$ cells, we found that the PX domain of p40^{phox} is much less critical in responses to PMA than the PX domain of p47^{phox} (supplemental Fig. 9), indicating that PMA, an analog of diacylglycerol, triggers predominantly p47^{phox}(PX)-dependent but p40^{phox}-independent oxidase activation, consistent with studies in p40^{phox}-deficient COS^{phox}FcγR cells and neutrophils (26, 28). Thus, the p40^{phox} and PI(3)P dependence in Nox2 activation is determined by stimulus (*e.g.* BIgG *versus* PMA).

Cho and Stahelin (58) described a general mechanism of membrane-protein interactions in which membrane adsorption of PX domain-containing proteins such as p47^{phox} and p40^{phox} (18, 56) is initially driven by nonspecific electrostatic interactions (between anionic lipids in membranes and cationic surfaces of proteins) and by diffusion, which is then followed by specific interaction with PIs and interfacial penetration (66) of hydrophobic and aromatic residues located near its respective binding site of PIs. Crystallographic studies on p40^{phox}, revealed that intramolecular PX-PB1 domain interactions are sterically inhibiting access of the PX domain with membrane-embedded PI(3)P, rather than completely masking the PI(3)P-binding site (13); in other words, the PX domain is able to access PI(3)P in certain conditions because three-dimensional positioning of membrane-embedded PI(3)P changes during phagosome formation. This speculation is supported by reports that full-length p40^{phox} binds to soluble PI(3)P to the same extent as the PX domain (39) and that full-length p40^{phox} binds to PI(3)P in surface plasmon resonance and lipid monolayer assays in which PI(3)P is flexible in the lipid monolayer (56). Considering our finding that p40^{phox} possessing the high affinity binding PX domain for PI(3)P accumulated on phagosomes (Fig. 4*A*), even if sterically inhibited, whereas FYVE-p40^{phox} possessing low affinity PI(3)P binding did not accumulate on phagosomes (Fig. 4*B*), the "semimasked" high affinity binding PX domain of p40^{phox} probably fulfills important missions during its translocation, including initiation of translocation.

Enhanced protein tyrosine phosphorylation by H_2O_2-induced inhibition of phosphotyrosine phosphatases has been reported (67, 68). In addition, it was reported that H_2O_2 directly induces conformational changes in proteins (69). In the present study, p40^{phox} tyrosine phosphorylation was not observed in response to H_2O_2 using anti-phosphotyrosine Ab (4G10) (data not shown), consistent with previous work (70), and conformational changes within p40^{phox} induced by H_2O_2 were observed by *in vitro* binding assays (Fig. 1, *F* and *G*). The other adaptor protein, p47^{phox}, showed no translocation to any membrane site in response to H_2O_2. Interestingly, PKCs, which are well known to phosphorylate p47^{phox} (10, 38, 71) and accumulate on phagosomes (38), are reported to be activated by H_2O_2 both on membranes and in the cytoplasm (72, 73). Thus, H_2O_2 may induce several positive feedback effects on both p40^{phox} and p47^{phox}, both on membranes and in the cytoplasm during the FcγR-mediated oxidative burst. In addition to this positive feedback mechanism of p40^{phox} directly acquiring PI(3)P binding capabilities by exposure to H_2O_2 (demonstrated in the present study) or by arachidonic acid (12), p40^{phox} can also indirectly acquire PI(3)P binding (Figs. 2*F* and 3, *C* and *F*) on targeted membranes in a p47^{phox}-dependent manner through its associations within the p47^{phox}-p67^{phox}-p40^{phox} complex.

Acknowledgments—We are thankful to Mr. Takeshi Hamada for his technical assistance. We also thank Dr. Y Irino and Prof. T Takenawa (Kobe University Graduate School of Medicine) for providing the 2xFYVE domain of mouse Hrs and the PH domain of human TAPP1.

REFERENCES

1. Quinn, M. T., and Gauss, K. A. (2004) *J. Leukoc. Biol.* **76,** 760–781
2. Sumimoto, H. (2008) *FEBS J.* **275,** 3249–3277
3. Leto, T. L., Morand, S., Hurt, D., and Ueyama, T. (2009) *Antioxid. Redox Signal.* **11,** 2607–2619
4. Borregaard, N., Heiple, J. M., Simons, E. R., and Clark, R. A. (1983) *J. Cell Biol.* **97,** 52–61
5. Lapouge, K., Smith, S. J., Groemping, Y., and Rittinger, K. (2002) *J. Biol. Chem.* **277,** 10121–10128
6. Segal, A. W., Heyworth, P. G., Cockcroft, S., and Barrowman, M. M. (1985) *Nature* **316,** 547–549
7. Bolscher, B. G., van Zwieten, R., Kramer, I. M., Weening, R. S., Verhoeven, A. J., and Roos, D. (1989) *J. Clin. Invest.* **83,** 757–763
8. Rotrosen, D., and Leto, T. L. (1990) *J. Biol. Chem.* **265,** 19910–19915
9. El-Benna, J., Dang, P. M., Gougerot-Pocidalo, M. A., Marie, J. C., and Braut-Boucher, F. (2009) *Exp. Mol. Med.* **41,** 217–225
10. Fontayne, A., Dang, P. M., Gougerot-Pocidalo, M. A., and El-Benna, J. (2002) *Biochemistry* **41,** 7743–7750
11. Boussetta, T., Gougerot-Pocidalo, M. A., Hayem, G., Ciappelloni, S., Raad, H., Arabi Derkawi, R., Bournier, O., Kroviarski, Y., Zhou, X. Z., Malter, J. S., Lu, P. K., Bartegi, A., Dang, P. M., and El-Benna, J. (2010) *Blood* **116,** 5795–5802
12. Ueyama, T., Tatsuno, T., Kawasaki, T., Tsujibe, S., Shirai, Y., Sumimoto, H., Leto, T. L., and Saito, N. (2007) *Mol. Biol. Cell* **18,** 441–454
13. Honbou, K., Minakami, R., Yuzawa, S., Takeya, R., Suzuki, N. N., Kamakura, S., Sumimoto, H., and Inagaki, F. (2007) *EMBO J.* **26,** 1176–1186
14. Ellson, C. D., Anderson, K. E., Morgan, G., Chilvers, E. R., Lipp, P., Stephens, L. R., and Hawkins, P. T. (2001) *Curr. Biol.* **11,** 1631–1635
15. Vieira, O. V., Botelho, R. J., Rameh, L., Brachmann, S. M., Matsuo, T., Davidson, H. W., Schreiber, A., Backer, J. M., Cantley, L. C., and Grinstein, S. (2001) *J. Cell Biol.* **155,** 19–25
16. Gillooly, D. J., Simonsen, A., and Stenmark, H. (2001) *J. Cell Biol.* **155,** 15–17
17. Gu, Y., Filippi, M. D., Cancelas, J. A., Siefring, J. E., Williams, E. P., Jasti, A. C., Harris, C. E., Lee, A. W., Prabhakar, R., Atkinson, S. J., Kwiatkowski, D. J., and Williams, D. A. (2003) *Science* **302,** 445–449
18. Karathanassis, D., Stahelin, R. V., Bravo, J., Perisic, O., Pacold, C. M., Cho, W., and Williams, R. L. (2002) *EMBO J.* **21,** 5057–5068
19. Sumimoto, H., Kage, Y., Nunoi, H., Sasaki, H., Nose, T., Fukumaki, Y., Ohno, M., Minakami, S., and Takeshige, K. (1994) *Proc. Natl. Acad. Sci. U.S.A.* **91,** 5345–5349
20. Leto, T. L., Adams, A. G., and de Mendez, I. (1994) *Proc. Natl. Acad. Sci. U.S.A.* **91,** 10650–10654
21. Heyworth, P. G., Curnutte, J. T., Nauseef, W. M., Volpp, B. D., Pearson, D. W., Rosen, H., and Clark, R. A. (1991) *J. Clin. Invest.* **87,** 352–356
22. Dusi, S., Donini, M., and Rossi, F. (1996) *Biochem. J.* **314,** 409–412
23. Allen, L. A., DeLeo, F. R., Gallois, A., Toyoshima, S., Suzuki, K., and Nauseef, W. M. (1999) *Blood* **93,** 3521–3530
24. Ellson, C. D., Davidson, K., Ferguson, G. J., O'Connor, R., Stephens, L. R., and Hawkins, P. T. (2006) *J. Exp. Med.* **203,** 1927–1937
25. Ellson, C., Davidson, K., Anderson, K., Stephens, L. R., and Hawkins, P. T. (2006) *EMBO J.* **25,** 4468–4478
26. Suh, C. I., Stull, N. D., Li, X. J., Tian, W., Price, M. O., Grinstein, S., Yaffe, M. B., Atkinson, S., and Dinauer, M. C. (2006) *J. Exp. Med.* **203,** 1915–1925
27. Ueyama, T., Kusakabe, T., Karasawa, S., Kawasaki, T., Shimizu, A., Son, J., Leto, T. L., Miyawaki, A., and Saito, N. (2008) *J. Immunol.* **181,** 629–640
28. Matute, J. D., Arias, A. A., Wright, N. A., Wrobel, I., Waterhouse, C. C., Li, X. J., Marchal, C. C., Stull, N. D., Lewis, D. B., Steele, M., Kellner, J. D., Yu, W., Meroueh, S. O., Nauseef, W. M., and Dinauer, M. C. (2009) *Blood* **114,** 3309–3315
29. Kuribayashi, F., Nunoi, H., Wakamatsu, K., Tsunawaki, S., Sato, K., Ito, T., and Sumimoto, H. (2002) *EMBO J.* **21,** 6312–6320
30. Chen, J., He, R., Minshall, R. D., Dinauer, M. C., and Ye, R. D. (2007) *J. Biol. Chem.* **282,** 30273–30284
31. Bissonnette, S. A., Glazier, C. M., Stewart, M. Q., Brown, G. E., Ellson, C. D., and Yaffe, M. B. (2008) *J. Biol. Chem.* **283,** 2108–2119
32. Tian, W., Li, X. J., Stull, N. D., Ming, W., Suh, C. I., Bissonnette, S. A., Yaffe, M. B., Grinstein, S., Atkinson, S. J., and Dinauer, M. C. (2008) *Blood* **112,** 3867–3877
33. de Mendez, I., Adams, A. G., Sokolic, R. A., Malech, H. L., and Leto, T. L. (1996) *EMBO J.* **15,** 1211–1220
34. Sathyamoorthy, M., de Mendez, I., Adams, A. G., and Leto, T. L. (1997) *J. Biol. Chem.* **272,** 9141–9146
35. Verhoeven, A. J., Bolscher, B. G., Meerhof, L. J., van Zwieten, R., Keijer, J., Weening, R. S., and Roos, D. (1989) *Blood* **73,** 1686–1694
36. Ueyama, T., Eto, M., Kami, K., Tatsuno, T., Kobayashi, T., Shirai, Y., Lennartz, M. R., Takeya, R., Sumimoto, H., and Saito, N. (2005) *J. Immunol.* **175,** 2381–2390
37. Ueyama, T., Geiszt, M., and Leto, T. L. (2006) *Mol. Cell. Biol.* **26,** 2160–2174
38. Ueyama, T., Lennartz, M. R., Noda, Y., Kobayashi, T., Shirai, Y., Rikitake, K., Yamasaki, T., Hayashi, S., Sakai, N., Seguchi, H., Sawada, M., Sumimoto, H., and Saito, N. (2004) *J. Immunol.* **173,** 4582–4589
39. Bravo, J., Karathanassis, D., Pacold, C. M., Pacold, M. E., Ellson, C. D., Anderson, K. E., Butler, P. J., Lavenir, I., Perisic, O., Hawkins, P. T., Stephens, L., and Williams, R. L. (2001) *Mol. Cell* **8,** 829–839
40. Ueyama, T., Lekstrom, K., Tsujibe, S., Saito, N., and Leto, T. L. (2007) *Free Radic. Biol. Med.* **42,** 180–190
41. Furutani, M., Tsujita, K., Itoh, T., Ijuin, T., and Takenawa, T. (2006) *Anal. Biochem.* **355,** 8–18
42. Larsen, E. C., Ueyama, T., Brannock, P. M., Shirai, Y., Saito, N., Larsson, C., Loegering, D., Weber, P. B., and Lennartz, M. R. (2002) *J. Cell Biol.* **159,** 939–944
43. Casbon, A. J., Allen, L. A., Dunn, K. W., and Dinauer, M. C. (2009) *J. Immunol.* **182,** 2325–2339
44. Choy, E., Chiu, V. K., Silletti, J., Feoktistov, M., Morimoto, T., Michaelson, D., Ivanov, I. E., and Philips, M. R. (1999) *Cell* **98,** 69–80
45. Miyano, K., Ogasawara, S., Han, C. H., Fukuda, H., and Tamura, M. (2001) *Biochemistry* **40,** 14089–14097
46. Alloul, N., Gorzalczany, Y., Itan, M., Sigal, N., and Pick, E. (2001) *Biochemistry* **40,** 14557–14566
47. Lindmo, K., and Stenmark, H. (2006) *J. Cell Sci.* **119,** 605–614
48. Seaman, M. N. (2008) *Cell. Mol. Life Sci.* **65,** 2842–2858
49. Bonifacino, J. S., and Rojas, R. (2006) *Nat. Rev. Mol. Cell Biol.* **7,** 568–579
50. Ago, T., Kuribayashi, F., Hiroaki, H., Takeya, R., Ito, T., Kohda, D., and Sumimoto, H. (2003) *Proc. Natl. Acad. Sci. U.S.A.* **100,** 4474–4479
51. Cheng, G., and Lambeth, J. D. (2004) *J. Biol. Chem.* **279,** 4737–4742
52. Blatner, N. R., Stahelin, R. V., Diraviyam, K., Hawkins, P. T., Hong, W., Murray, D., and Cho, W. (2004) *J. Biol. Chem.* **279,** 53818–53827
53. Gillooly, D. J., Morrow, I. C., Lindsay, M., Gould, R., Bryant, N. J., Gaullier, J. M., Parton, R. G., and Stenmark, H. (2000) *EMBO J.* **19,** 4577–4588
54. Mao, Y., Nickitenko, A., Duan, X., Lloyd, T. E., Wu, M. N., Bellen, H., and Quiocho, F. A. (2000) *Cell* **100,** 447–456
55. Kutateladze, T. G. (2007) *Prog. Lipid Res.* **46,** 315–327
56. Stahelin, R. V., Burian, A., Bruzik, K. S., Murray, D., and Cho, W. (2003) *J. Biol. Chem.* **278,** 14469–14479
57. Stahelin, R. V., Long, F., Diraviyam, K., Bruzik, K. S., Murray, D., and Cho, W. (2002) *J. Biol. Chem.* **277,** 26379–26388

58. Cho, W., and Stahelin, R. V. (2005) *Annu. Rev. Biophys. Biomol. Struct.* **34,** 119–151
59. Cheng, G., Ritsick, D., and Lambeth, J. D. (2004) *J. Biol. Chem.* **279,** 34250–34255
60. Ago, T., Nunoi, H., Ito, T., and Sumimoto, H. (1999) *J. Biol. Chem.* **274,** 33644–33653
61. Kanai, F., Liu, H., Field, S. J., Akbary, H., Matsuo, T., Brown, G. E., Cantley, L. C., and Yaffe, M. B. (2001) *Nat. Cell Biol.* **3,** 675–678
62. van den Berg, J. M., van Koppen, E., Ahlin, A., Belohradsky, B. H., Bernatowska, E., Corbeel, L., Español, T., Fischer, A., Kurenko-Deptuch, M., Mouy, R., Petropoulou, T., Roesler, J., Seger, R., Stasia, M. J., Valerius, N. H., Weening, R. S., Wolach, B., Roos, D., and Kuijpers, T. W. (2009) *PLoS ONE* **4,** e5234
63. Chessa, T. A., Anderson, K. E., Hu, Y., Xu, Q., Rausch, O., Stephens, L. R., and Hawkins, P. T. (2010) *Blood* **116,** 6027–6036
64. Fan, L. M., Teng, L., and Li, J. M. (2009) *Arterioscler. Thromb. Vasc. Biol.* **29,** 1651–1656
65. Wientjes, F. B., Reeves, E. P., Soskic, V., Furthmayr, H., and Segal, A. W. (2001) *Biochem. Biophys. Res. Commun.* **289,** 382–388
66. Málková, S., Stahelin, R. V., Pingali, S. V., Cho, W., and Schlossman, M. L. (2006) *Biochemistry* **45,** 13566–13575
67. Rhee, S. G. (2006) *Science* **312,** 1882–1883
68. Tonks, N. K. (2006) *Nat. Rev. Mol. Cell Biol.* **7,** 833–846
69. Umada-Kajimoto, S., Yamamoto, T., Matsuzaki, H., and Kikkawa, U. (2006) *Biochem. Biophys. Res. Commun.* **341,** 101–107
70. Grandvaux, N., Elsen, S., and Vignais, P. V. (2001) *Biochem. Biophys. Res. Commun.* **287,** 1009–1016
71. Shiose, A., and Sumimoto, H. (2000) *J. Biol. Chem.* **275,** 13793–13801
72. Konishi, H., Tanaka, M., Takemura, Y., Matsuzaki, H., Ono, Y., Kikkawa, U., and Nishizuka, Y. (1997) *Proc. Natl. Acad. Sci. U.S.A.* **94,** 11233–11237
73. Ohmori, S., Shirai, Y., Sakai, N., Fujii, M., Konishi, H., Kikkawa, U., and Saito, N. (1998) *Mol. Cell. Biol.* **18,** 5263–5271